Multivariate optimization for extraction of 2-methylimidazole and 4-methylimidazole from *açaí*-based food products using polymeric ionic liquid-based sorbent coatings in solid-phase microextraction coupled to gas chromatography–mass spectrometry

Luis Eduardo SILVA NASCIMENTO[a,b], Bhawana THAPA[b], Wellington DA SILVA OLIVEIRA[c], Plínio RIBEIRO RODRIGUES[d], Helena TEIXEIRA GODOY[a], Jared L. ANDERSON[b*]

[a] Department of Food Science and Nutrition, School of Food Engineering, University of Campinas (UNICAMP), Rua Monteiro Lobato, 80, 13083-862, Campinas, SP, Brazil

[b] Department of Chemistry, Iowa State University, 2415 Osborn Drive, Ames, IA 50011, USA

[c] Reference Laboratory for Physical, Sensory and Statistics Analysis, Science and Food Quality Center, Institute of Food Technology (ITAL), Avenida Brasil 2880, 13070-178 Campinas, Sao Paulo, Brazil

[d] Department of Fundamental Chemistry, Institute of Chemistry, University of São Paulo (USP), Avenida Lineu Prestes, 748, 05508-000, Cidade Universitária, São Paulo, SP, Brazil

*** Corresponding author:**
Jared L. Anderson
Department of Chemistry
Iowa State University
1605 Gilman Hall
Ames, IA 50011
Tel.: +1 515-294-8356
E-mail address: andersoj@iastate.edu
ORCID: 0000-0001-6915-8752

Keywords

Central composite rotatable design; *Euterpe oleracea*; food analysis; food contaminant; plackett-burman design; SPME.

Abstract

In this study, polymeric ionic liquids featuring different functional moieties were applied as sorbent coatings in direct-immersion solid-phase microextraction (DI-SPME) for the extraction of 2-methylimidazole (2-MI) and 4-methylimidazole (4-MI) from *açaí*-based food products followed by gas chromatography-mass spectrometry (GC-MS) analysis. The analytical method was optimized using a sequential experimental design. Variables used in GC-MS such as desorption time, as well as for SPME-DI, including extraction time, extraction temperature, incubation time of extraction, amount of NaCl in the extract, and stirring rate, were optimized. The fitness-for-purpose of the method was verified by the linearity of matrix-matched calibration curves ($R^2 \geq 0.9921$), adequate recoveries (81.7–89.7 %), and precision (relative standard deviations ≤ 11.2 %). The method was applied to twenty-five samples of *açaí*-based food products. 4-MI was found in four samples whereas 2-MI was not detected above the limit of detection. The method was found to be suitable for quality control analysis.

1. INTRODUCTION

Açaí-based food products are derived from the edible parts of the *Euterpe oleracea* palm tree fruits. The largest cultivated area for these products is in the eastern Brazilian Amazon region. Over the past few years, *açaí*-based food products have experienced an expansion due to their increased sales within Brazil. Recently, another significant contributing factor has been the growing presence of these products within the

international market (CONAB, 2021).

The molecules 2-methylimidazole (2-MI) and 4-methylimidazole (4-MI) are process contaminants that may be present in *açaí*-based food products. Overall, contamination of foods by 2-MI and 4-MI occurs through the following two pathways: (1) the most likely source is when food is sweetened using guaraná syrup that contains caramel colorants E150c (Class III) and E150d (Class IV); (2) The other pathway involves the heating of carbohydrates and nitrogenous compounds. In the latter case, the pasteurization process leads to the formation of contaminants. However, the likelihood of this scenario is low, as the pasteurization process occurs within a short period of time preventing the formation of large amounts of these toxic compounds (Akbari et al., 2023).

The International Agency for Research on Cancer (IARC) has classified 2-MI and 4-MI as possibly carcinogenic to humans (IARC, 2023). Additionally, the European Food Safety Authority (EFSA) establishes acceptable daily intake (ADI) levels of 100 and 300 mg kg^{-1} body weight per day for 4-MI in caramel colorants Class III and Class IV, respectively (EFSA, 2011). Furthermore, the European Commission's regulations set limits of 200 and 250 mg of 4-MI per kg^{-1} for caramel colorants Class III and Class IV, respectively (EC, 2012). On the other hand, there are no regulations that establish limits for 2-MI. More restrictively, using the Cramer classification scheme, the toxicological threshold of concern (TTC) value is 90 μg per person per day for each compound (More et al., 2019).

Several methods have been proposed to determine 2-MI and 4-MI in foodstuffs. Due to their high polarity and low volatility, their analysis can be challenging in food matrices containing high water content, such as *açaí*-based food products. To overcome these challenges, derivatization steps have been used prior to gas chromatography (GC) and liquid chromatography (which commonly uses a polar column). However, these

sample preparation methods require laborious and time-consuming steps, in addition to the use of toxic solvents (Revelou et al., 2021). Approaches that are environmentally sustainable, such as green extraction methodologies that do not involve the use of toxic solvents or the production of by-products, have been applied in food analysis. Additionally, user-friendly and simplified methods are also highly sought after. In this context, microextraction techniques, including solid-phase microextraction (SPME), have been utilized for the determination of food contaminants (Pedersen-Bjergaard, 2019; Revelou et al., 2021).

Over the past few years, polymeric ionic liquids (PIL) have been explored as a new a class of sorbent coatings for SPME (Cagliero, Nan, et al., 2016; Meng et al., 2011; Zeger et al., 2022). Due to the tunability of their chemical structures, which often include different monomers and dicationic crosslinkers, these materials can provide unique selectivity owing to their affinity for different target analytes (Zeger et al., 2022). Additionally, studies have demonstrated that PIL-based SPME produces advantageous analytical results compared to other commercially available coatings (Cagliero, Ho, et al., 2016; Gionfriddo et al., 2018; Zeger et al., 2022). Furthermore, functionalizing PILs with polar and hydrogen-bonding-capable substituents increases their affinity towards highly polar analytes, resulting in improved selectivity and fulfillment of a gap left by commercial coatings (Yu et al., 2013).

The successful implementation of SPME requires careful evaluation of the factors that can influence extraction efficiency. Multivariate tools, namely Plackett-Burman (PB) and central composite rotatable design (CCRD), have thus been applied for this step because they provide optimal extraction conditions for all independent variables simultaneously investigated, in addition to providing information regarding their interactions. Also, multivariate methods require a lower number of runs, less time, and

resulting lower analysis costs compared to univariate optimization, which deals with one variable at a time. In this context, Derringer and Suich's tool is a statistical method that analyzes the ideal simultaneous extraction conditions for all studied analytes (Galindo et al., 2021; Oliveira et al., 2020).

To the best of our knowledge, no studies have addressed sequential multivariate optimization for the extraction of 2-MI and 4-MI from any food sample or for improving the extraction method's performance using PIL-based SPME. For this purpose, three imidazolium-based PIL sorbent coatings comprised of different functional moieties appended to the ionic liquid (IL) monomers and dicationic IL crosslinkers were examined. The aim of this study was to develop and validate a method for the quantitative analysis of 2-MI and 4-MI in *açaí*-based food products using PIL-based SPME assisted by multivariate optimization and combined with GC-MS. In addition, the developed method eliminates the need for any derivatization step, which commonly employed in the analysis of 2-MI and 4-MI by GC. The incidence of these analytes was investigated in twenty-five samples of *açaí*-based food products obtained from Brazil and the United States.

2. MATERIALS AND METHODS

2.1. Samples

Twenty-five samples of *açaí*-based food products were purchased from different manufacturers in Brazil and the United States. Table 1 displays in detail more information about each sample. The samples were kept frozen at −18 °C ± 2 °C until analysis. All samples were analyzed in triplicate.

For all steps involving analysis with a food matrix (sections: 2.3.2, 2.3.3, 2.3.4, and 2.5), it was used a representative blank sample formulated by mixing the samples

129 shown in Table 1, including *açaí* pulp, *açaí* with strawberry, *açaí* with banana, and *açaí*
130 with guaraná syrup in a ratio of 1:1:1:1 (w/w).
131
132 **Table 1**. Main ingredients and country of origin of analyzed *açaí*-based food products, as
133 well as their sample name.

Sample	Main ingredients*	Origin	Sample	Main ingredients*	Origin
A	*Açaí* pulp with strawberry	Brazil	N	*Açaí* pulp	Brazil
B	*Açaí* pulp with *guaraná*	Brazil	O	*Açaí* pulp	Brazil
C	*Açaí* pulp with strawberry	Brazil	P	*Açaí* pulp	U.S.
D	*Açaí* pulp with strawberry	Brazil	Q	*Açaí* pulp with *guaraná*	U.S.
E	*Açaí* pulp with *guaraná*	Brazil	R	*Açaí* pulp with *guaraná*	U.S.
F	*Açaí* pulp with *guaraná*	Brazil	S	*Açaí* pulp with *guaraná*	U.S.
G	*Açaí* pulp with strawberry	Brazil	T	*Açaí* pulp	U.S.
H	*Açaí* pulp with banana	Brazil	U	*Açaí* pulp	U.S.
I	*Açaí* pulp with banana	Brazil	V	*Açaí* pulp	U.S.
J	*Açaí* pulp with banana	Brazil	W	*Açaí* pulp	U.S.
K	*Açaí* pulp	Brazil	X	*Açaí* pulp	U.S.
L	*Açaí* pulp	Brazil	Y	*Açaí* pulp	U.S.
M	*Açaí* pulp	Brazil	-	-	-

134 * Classification was printed on the packaging of each sample. All samples contained
135 *guaraná* syrup among their ingredients.
136
137 **2.2. Chemicals**
138 Ethyl acetate (ACS reagent, ≥ 99.5 %) was purchased from Millipore-Sigma (St.
139 Louis, MO, USA). Lithium bis[(trifluoromethyl)sulfonyl]imide ($LiNTf_2$) was obtained

from Synquest Laboratories (Alachua, FL, USA). Silver nitrate, hydrogen peroxide ≥ 29%, chloroform ≤ 99.8%, sodium chloride, and acetone ≥ 99.5 were purchased from Fisher Scientific (Pittsburgh, PA, USA). Dimethyl sulfoxide-d6 (D, 99.9%) was purchased from Cambridge Isotope Laboratories, Inc. (Tewksbury, MA, USA). 2-hydroxy-2-methylpropiophenone (DAROCUR 1173) was purchased from TCI (Portland, OR, USA). Methanol HPLC grade ≥ 99.9%, acetonitrile (HPLC grade), acrylonitrile ≥ 99.9, 1-vinylimidazole ≥ 99 %, 1,12-dibromododecane 98%, 10-bromodecanoic acid 95%, 10-bromo-1-decanol 90%, imidazole 99%, vinyltrimethoxysilane 98%, 2-methylimidazole 99%, 4(5) methylimidazole 98%, and (±)-menthol were purchased from Sigma-Aldrich® (St. Louis, MO, USA). Super elastic nitinol wire (external diameter of 127 µm) was acquired from Component Supply (Sparta, TN, USA). Polyacrylate SPME fibers (85 µm) were purchased from Supelco (St. Louis, MO, USA). Epoxy adhesive paste (Resin type epoxy and hardener) was purchased from J-B WELD (Sulphur Springs, TX, USA). A multi-analyte working solution containing the native standards (2-MI and 4-MI) was prepared using Milli-Q® water at a concentration of 100 µg mL^{-1}. The internal standard (IS), (±)-menthol, was prepared as a working solution at a concentration of 10 µg mL^{-1}. The Milli-Q® water was obtained from the Simplicity® UV Water Purification System (Millipore SAS, Molsheim, GES, France).

2.3. Sample preparation

2.3.1. Preparation of PIL-based SPME fibers

In this study, three different PIL-based SPME fibers were developed and are denoted as PIL 1, PIL 2 and PIL 3 as shown in Table 2. The PIL 1 fiber was based on the IL monomer 1-vinyl-3-(10-hydroxydecyl)imidazolium bis[(trifluoromethyl)sulfonyl]imide [NTf_2^-]. The PIL 2 and PIL 3 fibers were based on

the 1-vinyl-3-(9-carboxynonyl)imidazolium [NTf_2^-] IL monomer. Two different crosslinkers were used, 1,12-di(3-vinylbenzylimidazolium)dodecane 2[NTf_2^-] for PIL 1 and PIL 2, and 1,12-di(3-vinylimidazolium)dodecane 2[NTf_2^-] for PIL 3. All reactions used to prepare the ILs were carried out under the same previously reported conditions (Anderson & Armstrong, 2005; Cagliero, Nan, et al., 2016; Joshi et al., 2014).

Table 2. Structural composition, approximate film thickness, and phase volume of the PIL-based sorbent coatings examined in this study.

Fiber	IL monomer	IL crosslinker	Approximate film thickness (μm)[a]	Volume (μL)[b,c]
	Structural composition			
PIL1	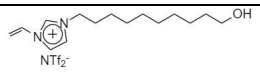 ([$VC_{10}OHIM^+$] [NTf_2^-])	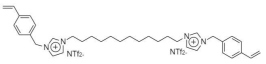 ([$(VBIM)_2C_{12}^{+2}$]2[NTf_2^-])	86 ± 10	0.17 ± 0.01
PIL 2	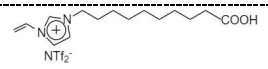 ([$VC_9COOHIM^+$] [NTf_2^-])	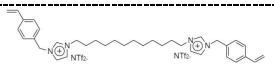 ([$(VBIM)_2C_{12}^{+2}$]2[NTf_2^-])	68 ± 8	0.14 ± 0.01
PIL3	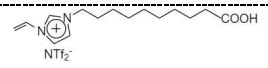 ([$VC_9COOHIM^+$] [NTf_2^-])	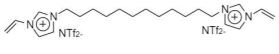 ([$(VIM)_2C_{12}^{+2}$]2[NTf_2^-])	66 ± 11	0.14 ± 0.01

PIL: polymeric ionic liquid, IL: ionic liquid

[a]average calculated using n = 10 samples, [b]the procedure used for calculation and a representative optical micrograph of the PIL-based fiber droplet (Figure S5) are provided in section 2.3.1.3. [c]average calculated using n = 3 samples.

Preparation of the PIL-based fibers was performed in the following three steps: (1) synthesis of the IL monomers and IL crosslinkers, (2) derivatization of the nitinol

wires, and (3) *on fiber* UV co-polymerization of the IL monomer and IL crosslinker. ^{1}H NMR spectra (Figure S1, S2, S3, and S4) are provided in Supplementary Material.

2.3.1.1. Derivatization of nitinol wire

Nitinol wires were cut into 1.5 cm segments and immersed in boiling hydrogen peroxide (30% w/w) for 3 h at 72 °C to derivatize the substrate surface with active hydroxyl moieties (Ti–OH). The wires were then dried overnight in a vacuum oven at 80 °C. The oxidized wires were subsequently functionalized with vinyltrimethoxysilane (VTMS) at 85 °C for 5 h to chemically bond the organosilane (vinyl moieties) to the surface of the alloy (Ho et al., 2014). The free vinyl groups on the surface of the functionalized nitinol acted as active points to chemically attach the PIL to the solid support. After functionalization, the nitinol wires were then glued onto a commercial SPME assembly (Ho et al., 2014).

2.3.1.2. On fiber UV co-polymerization of the polymeric ionic liquid

The homemade SPME device was constructed by using a previously published procedure (Ho et al., 2014). Functionalized nitinol was attached to SPME holder using a mix of epoxy adhesive paste, including resin (steel) and hardener mixed at a ratio of 1:1. A full cure was reached for 24 hours at room temperature. Next, the functionalized nitinol was cleaned with a soft paper napkin with acetone and dried in hot air for 20 seconds before the IL was applied. A 1.3 cm length of the nitinol functionalized with VTMS was then dip-coated with a solvent-free mixture containing the IL monomer, IL crosslinker (50% w/w, with respect to the monomer) and the photo-initiator DAROCUR 1173 (5% w/w, with respect to the monomer) as a free radical initiator. This mixture was previously prepared under agitation for 5 min at 35 °C ± 1 °C. Afterwards, the fiber was exposed to

360 nm UV light for 2 h min using an RPR-100 UV photochemical reactor with a spinning carousel (Southern New England Ultraviolet Company, Bradford, CT, USA). The stability of the crosslinked PIL-based coatings (fiber) was investigated by adding the fiber first to 20% methanol for 5 min, followed by another 10 min and finally for 15 min. The coating must not dissolve for the fiber to be considered efficient for injection to the GC-MS. The fiber was conditioned twice at 220 °C for 30 min.

2.3.1.3. Calculation of the volumes of sorbent coatings

Since PIL sorbent coatings often tend to form droplets, and to calculate the volumes of sorbent coatings, the actual volumes of all droplets were summed. Each droplet was ellipsoid in shape and thus their volumes were calculated first using the following formula for the volume of ellipsoid (Ve):

$Ve = 4/3*\pi*a*b*c$, where $a = l/2$ (l = length of ellipsoid), $b = c = d/2$ (d = diameter of ellipsoid)

The volume of the nitinol wire (core of the fiber, Vc) within each ellipsoid was then calculated using the formula for cylinder:

$Vc = \pi*r^2*h$, where h = length of wire within the ellipsoid and $r = 127/2$ (the diameter of nitinol wire was 127 µm)

The actual volume of each droplet (Vd) was then calculated by subtracting the volume of nitinol wire by the volume of ellipsoid ($Vd = Ve - Vc$).

Upon calculation of actual volumes for all droplets, the total volume of sorbent was calculated by summing the actual volumes of all droplets.

2.3.1.4. Optical microscopy analysis

Microscopy images were obtained using a 10x infinite plan achromatic objective lens fitted onto an LB-241 Biological Digital Microscope with a BCN2F-0.37× 23.2 mm Eyepiece Adapter connected to an LC-35 - 5MP USB2.0 Graphics Accelerated Microscope Camera (LABOMED Inc., Los Angeles, CA, USA). Image acquisition was obtained using the software Capture 2.1.

2.3.2. Fiber selection for extraction of 2-MI and 4-MI

The extraction efficiency test was carried out using the variables fitted in level -1 of the Plackett–Burman (PB) Design (Table S1). Briefly, assessment of the fibers was performed using the following variables: extraction time (30 min), extraction temperature (30 °C), incubation time (5 min), NaCl (5% - w/v), desorption time (1 min), and stirring rate (200 RPM). Table 2 describes the chemical composition of the PIL-based fibers. The extraction procedure was performed similarly as reported in section 2.3.4. A commercial polyacrylate (PA) fiber was used for comparison purposes.

2.3.3. Multivariate optimization

The conditions employed to extract 2-MI and 4-MI from *açaí*-based food products were optimized using direct-immersion solid-phase microextraction (DI-SPME) through the PB, CCRD, and Derringer and Suich designs to identify the best extraction condition. For this, the sample was spiked with native standards at a concentration of 1 mg kg^{-1} through the addition of 10 µL of the multi-analyte working solution. Additionally, the IS

was added at a concentration of 0.1 mg kg^{-1} using 10 µL of its respective working solution. As result, optimization was based on the peak area values for each compound. In summary, PB design was used to determine the most important independent variables that impact the extraction of these compounds. The following variables were evaluated at two levels, high (+1) and low (−1), including incubation time (min), extraction time (min), extraction temperature (°C), amount of NaCl (%, w/v), stirring rate (RPM), and desorption time (min). Table S1 shows the design matrix with the coded and real values for the studied variables. The experimental design included 12 trials and 3 central points, resulting in 15 independent trials (Table S2). The variables were analyzed using 10% of significance, in order to minimize the risk of excluding an important variable in the next step (Galindo et al., 2021).

Subsequently, variables that showed a significant effect were optimized through a CCRD ($p<0.05$). The CCRD was based on a 2^3 factorial design evaluated at different levels, low level (−1), central point (0), high level (+1), and axial points (−α and +α) to determine the optimized extraction conditions (Table S3). The experiment was performed randomly in an effort to mitigate the effect of nonessential variables (Table S4).

Finally, the desirability function proposed by Derringer and Suich (Derringer & Suich, 1980) was used to obtain the best response simultaneously for both compounds. This function is based on individual responses of each compound and then combined into their global desirability function. This desirability is based on maximization of analyte extraction and is measured in the range from 0.0 to 1.0 values where 0.0 indicates an undesirable value and 1.0 indicates a very desirable value. Furthermore, Derringer and Suich's tool (D&S) uses the experimental results obtained from CCRD to perform its statistical analyses. The mathematical models indicated by the desirability function were experimentally validated and used to extract the compounds proposed in this study.

In summary, CCRD is used to individually determine the best extraction conditions for each investigated analyte, while D&S is employed to achieve the optimal extraction conditions for all analytes simultaneously.

The PB and CCRD results were processed by the Protimiza Experimental Design software (Protimiza Experimental Design, Campinas, SP, Brazil). The experiments obtained from Derringer and Suich's tool were conducted using Design Expert 6.0 software (Stat-Ease, Minneapolis, MN, USA).

2.3.4. Extraction method

The optimized extraction condition involved the following steps: 1 g of homogenized *açaí*-based food product sample was weighed into a 20 mL glass vial. Then, 15 mL of water was added followed by vortexing for 30 s. For the salting out effect, 0.75 g of NaCl was added with subsequent stirring for 30 s. The vial containing the sample was incubated for 5 min. The incubation and extraction temperature were 57.1 ºC. In addition, the extraction condition was obtained using a stirring rate of 567 RPM for 100 min and thermal desorption of the analytes in the GC inlet for 3 min.

2.4. Chromatographic conditions and mass spectrometry

For 2-MI and 4-MI quantification, gas chromatograph-mass spectrometry (GC–MS) (Agilent, Santa Clara, CA, USA) was used. The system consisted of a 7890B GC coupled with a single quadrupole 5977A (Agilent, Santa Clara, CA, USA) mass spectrometer with an electron ionization (EI) chamber. GC separation was achieved on an Agilent J&W HP-FFAP capillary column (30m × 0.25 mm ID × 0.25 µm film thickness, Agilent, Santa Clara, CA, USA). The oven temperature was programmed initially at 60 °C for 0.9 min, increased to 140 °C at 10 °C min^{-1} and held for 1 min,

304 ramped to 170 °C at 2 °C min^{-1}, and finally ramped to 230 °C at 30 °C min^{-1} and held
305 for 5 min, with a total run of 31.9 min. Ultra-high purity helium (Matheson, CO, USA)
306 was used as the carrier gas at 1.0 mL min^{-1}. The GC inlet was maintained at 240 °C in
307 spitless mode (100 ml min^{-1} at 1 min). The electron ionization energy was 70 eV. The
308 temperatures of the MS transfer line, ion source, and the MS quadrupole were set to 235
309 °C, 235 °C, and 180 °C, respectively. System control and data acquisition were performed
310 in MassHunter software, version B.07.00. (Agilent, Santa Clara, CA, USA).

311 Analyses were conducted with a solvent delay of 4 min. Data were initially
312 acquired in SCAN mode (mass range: 50–350 *m*/*z*) to locate and identify 2-MI, 4-MI, and
313 the IS in the samples. Selected ion monitoring (SIM) was used for analysis of each
314 compound. Three specific ions were selected for the analysis of each compound,
315 including one as the target ion (quantification: 82 m/z for 2-MI and 4-MI) and two as
316 qualifying ions (qualifier ion: 81 and 54 *m*/*z* for 2-MI and 4-MI). The analytes were
317 confirmed by comparing the ions and retention times using their commercial standards.
318 Quantification was performed by internal standardization including one quantifier ion and
319 two as qualifying ions (target ion: 71 *m*/*z*, qualifier ion: 81 and 95 *m*/*z*).

320

321 **2.5. In-house validation**

322 Validation of the optimized method was assessed considering the requirements of
323 the Commission Decision 2002/657/EC (EC, 2002). The method was validated for limit
324 of detection (LOD), limit of quantification (LOQ), linearity, recovery, matrix effects, and
325 precision intra- and inter-days.

326 LOD and LOQ were defined as the lowest concentration in a spiked blank sample
327 that achieved signal-to-noise ratios of 3:1 and 10:1, respectively. Linearity was evaluated
328 in solvent and matrix-matched calibration curves where seven calibration levels (with

329 equidistant points of 20.83) were used with concentrations ranging from 75 to 200 μg
330 kg^{-1}. Recovery (%) assays were performed in three concentration levels (LOQ, 100, and
331 200 μg k^{-1}) using six replicates. The matrix effect (ME) was calculated for each
332 compound, where ME(%) = Matrix Effect (%) = [(matrix-matched calibration slope –
333 solvent calibration slope)/solvent calibration slope] x 100 (Nascimento et al., 2023).
334 Precision was performed using a spiked blank sample, at three concentration
335 levels (LOQ, 100, and 200 μg kg^{-1}) in triplicate for repeatability (intra-day precision) and
336 reproducibility (inter-day precision – three days) studies. The precision results were
337 expressed as relative standard deviation (%RSD).
338
339 **2.6. Practical aspects and green assessment of the analytical method**
340 In order to evaluate the environmental sustainability and practicality of the
341 analytical methodology employed in this study, the Green Analytical Procedure Index
342 (GABI) (Płotka-Wasylka, 2018) and the Blue Applicability Grade Index (BAGI)
343 (Manousi et al., 2023), respectively, were utilized. GABI assesses parameters ranging
344 from sample collection to final determination, utilizing five pentagrams to gauge the
345 environmental impact of each segment of the analytical procedure. Meanwhile, BAGI
346 assigns scores to a pictogram, reflecting aspects related to the practicality and
347 applicability of an analytical method. This pictogram delineates the strengths and
348 weaknesses of procedural steps in terms of practicality and applicability. To analyze its
349 results, this index is categorized into 10 groups that scrutinize analytical determinations
350 and sample preparation steps.
351
352 **3. RESULTS AND DISCUSSION**
353 **3.1. Structural design of crosslinked PIL-based sorbent coatings**

PIL-based sorbent coatings comprised of different combinations of IL monomers and crosslinkers were synthesized to examine their selectivity towards 2-MI and 4-MI. Their performance was then compared with a commercial PA fiber. The composition of the PIL sorbent coatings tested in this study is provided in Table 2. In an effort to enhance the polarity of the sorbent coatings, various IL monomers were tailored to incorporate polar groups to the terminal end of the alkyl chain. Polar compounds have been previously shown to be readily extracted when the PIL cationic moiety contains polar substituent groups (Pacheco-Fernández et al., 2019). Thus, a hydroxyl moiety was introduced to PIL 1, while carboxylic acid moieties were incorporated into PIL 2 and PIL 3, thereby permitting an examination of the effects of hydrophilic interactions on the extraction selectivity of these analytes. Furthermore, the crosslinker composition featured vinyl benzyl moieties in PIL 1 and PIL 2, with a vinyl moiety present in PIL 3.

Aromatic moieties (vinyl benzyl groups) were introduced into the crosslinker of PIL 1 and PIL 2, as this functional group may enhance specificity in the extraction of aromatic compounds. This interaction occurs by enhancing π-π interactions between aromatic analytes and the vinyl benzyl-terminated PIL (Pacheco-Fernández et al., 2016; Yu et al., 2016). Additionally, the $[NTf_2]^-$ anion was incorporated into all PIL sorbent coatings to exploit its capability in the extraction of polar analytes, while also providing high thermal stability. This latter characteristic is particularly desirable as the GC inlet operates at high temperatures (Ho et al., 2011; Meng et al., 2011)

Lastly, the analytes 2-MI (pKa 7.86) and 4-MI (pKa 7.51) are classified as weak bases (basic analytes) and exhibit hydrophilic characteristics (log K_{ow} = 0.24 for 2-MI and 0.23 for 4-MI) (PubChem, 2023). Therefore, enhancing interactions between the functionalized PIL and basic analytes can occur through hydrogen bonding interactions (Yu et al., 2016). This interaction is favored due to the presence of an unsubstituted

379 nitrogen in imidazole, which acts as a hydrogen-bond acceptor for the N-H group
380 (Hachuła et al., 2010). Consequently, the incorporation of hydroxyl and carboxylic acid
381 moieties into the PIL chemical structure facilitates hydrogen bonding interactions,
382 leading to potential improvement in hydrogen bonding acidity (Yu et al., 2016).
383

384 **3.2. Fiber selection for extraction of 2-MI and 4-MI**

385 Because the phase volume values used for preparing the PIL fibers were different,
386 the results could potentially show misleading analyte extraction efficiencies due to these
387 variations. Therefore, normalization was employed to adjust the extraction efficiency
388 based on the sorbent phase volume using the following equation: n = peak area / phase
389 volume value.

390 Figure 1 depicts both non-normalized and normalized data with results expressed
391 as chromatographic peak area. For normalization of the PA fiber, the phase volume was
392 determined based on information available in the literature for coating this type of fiber.
393 A phase volume value of 0.543 µL was used for the PA coating based on previous
394 reported data (Shirey, 2012).
395

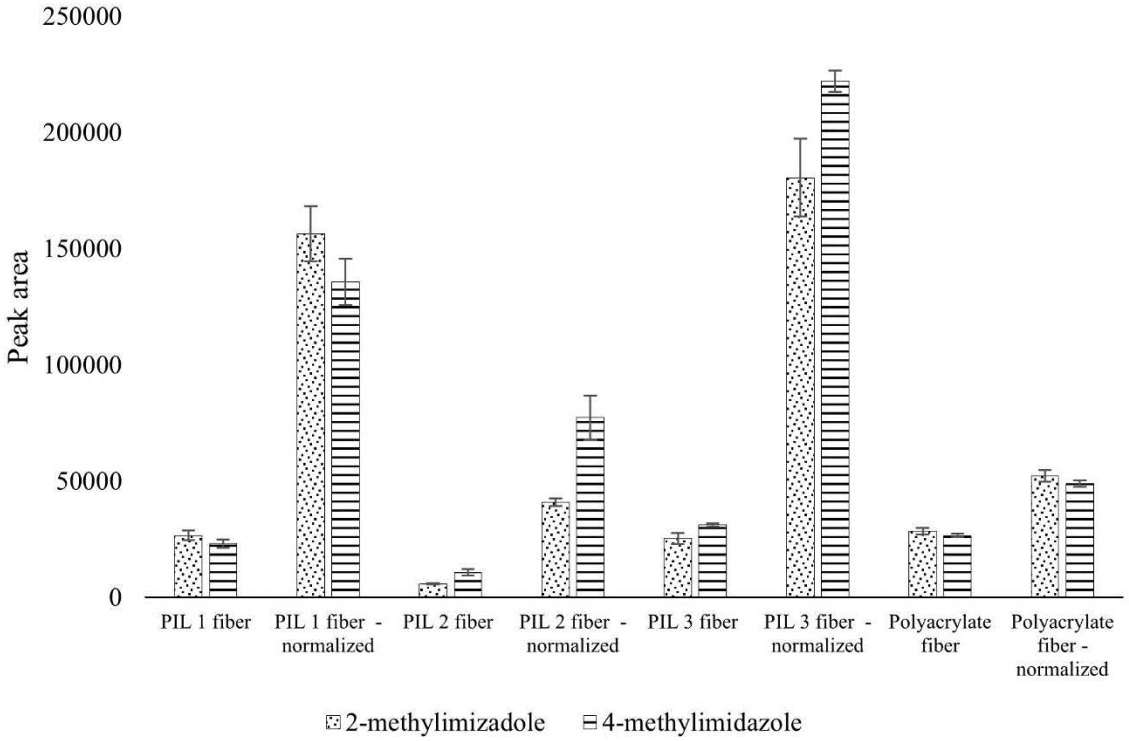

396

397 **Figure 1**. Normalized and non-normalized bar graphs showing a comparison of extraction
398 efficiency of each fiber (three PIL fibers and one commercial PA fiber) for 2-
399 methylimidazole and 4-methylimidazole.

400 PIL: Polymeric Ionic Liquid

401

402 Observing the chart, it is possible to note an increase in extraction efficiency when
403 comparing normalized and non-normalized data, which was more obvious for the PIL
404 fibers. This phenomenon occurs because the PIL fibers offered greater extraction
405 efficiency per phase volume compared to the PA fiber. Regarding the difference among
406 the phase volume of different PIL fibers, this was already expected since they were
407 manufactured in-house. Therefore, some variations can be expected during fiber
408 preparation.

409 Taking into account the normalized data, the PA fiber showed lower extraction
410 efficiency than those obtained from PIL fibers for both analytes (except for 2-MI, which
411 obtained higher extraction efficient only regarding PIL 2 fiber), even though the PA fiber

had the highest phase volume (approximately three times greater than that used for the PIL fibers). This phenomenon is likely due to the presence of interferents, usually found in complex matrices like food samples, that may hinder the performance of the PA fiber and resulting in analytical issues such as low sensitivity, when compared to PIL fibers (Pacheco-Fernández et al., 2019). Furthermore, the results showed that the PIL-based absorbent coating is more efficient than the commercial fiber absorbent coating tested in this work. Consequently, it is possible to infer that the extraction of these analytes per unit of phase volume is higher in the PIL-based fiber, which highlights the performance of these materials compared to that already found in the market.

Regarding the non-normalized data, 4-MI was best extracted using PIL 3. On the other hand, 2-MI was more effectively extracted using the PA fiber. Despite the fact that 2-MI is considered possibly carcinogenic to humans (IARC, 2023), neither the EFSA nor the European Commission Regulation has yet established a threshold for this analyte. As a result, the regulation only specifies 4-MI. For this reason, PIL 3 was selected for the subsequent step (multivariate optimization) and for performing analytical validation of the method, as it demonstrated the best performance in the extraction of 4-MI (EC, 2012; EFSA, 2011).

As shown in Figure 1, the extraction efficiencies of both analytes varied based on the type of fiber used. Given that absorption is the primary extraction mechanism of both the PA and PIL fibers, the analytes can readily partition into the sorbent materials (Carriço et al., 2020). As a result, the concentration of each analyte (despite them being isomers) may be influenced by their competition for sorbent active sites. Additionally, the coating thickness influences the absorption capacity of the fibers (Carriço et al., 2020).

For the 2-MI, the fibers that provided the best extraction response (considering the data without normalization) followed the decreasing order: PA fiber > PIL 1 > PIL 3

437 > PIL 2. Among the PIL fibers, the sorbent coating featuring a hydroxyl group (PIL 1)
438 exhibited superior extraction efficiency compared to the other PIL fibers. Furthermore,
439 this fiber possessed a greater film thickness and approximately 0.21 times more sorbent
440 volume than the other PIL fibers, as indicated in Table 2. Therefore, it can be inferred
441 that PIL 1 had a higher amount of PIL, resulting in improved extraction efficiency.
442 Similar findings were previously demonstrated by Cagliero and co-workers, who
443 investigated different IL monomers incorporating either a hydroxy group or a carboxylic
444 group appended to the IL cation for the extraction of the polar acrylamide analyte. Their
445 work concluded that the hydroxy moiety exhibited superior extraction performance
446 compared to the carboxylic moiety (Cagliero, Ho, et al., 2016).

447 Concerning 4-MI, the extraction efficiency (considering the non-normalized data)
448 was observed in the following decreasing order: PIL 3 > PA > PIL 1 > PIL 2. PIL 3
449 featured a carboxylic acid moiety and the observed data aligns with a study that
450 demonstrated superior performance for the carboxylic acid moiety over the hydroxy
451 moiety for the extraction of polar analytes (Nacham et al., 2016).

452

453 **3.3. Multivariate optimization**

454 A multivariate sequential design was selected to optimize the extraction method
455 using the PIL 3 fiber. When using a factor-by-factor approach in optimization, a
456 significant amount of information can be missing during the analysis process as this
457 method does not allow for the simultaneous assessment of interactions among all
458 independent variables. Therefore, multivariate optimization was applied and contains
459 features that yield better statistical results, such as the concurrent occurrence of
460 interactions between factors when compared to factor-by-factor optimization. The

sequential optimization employed in this study consisted of the following three steps: (1) PB; (2) CCRD; and (3) Derringer & Suich's tools.

3.3.1. Plackett-Burman design (PB)

The PB assay was employed to assess the impact of each independent variable on the extraction efficiency of the investigated analytes. The experiment was performed with a blank sample spiked with 2-MI and 4-MI at 1 mg kg^{-1}. PB screening revealed that among the studied factors, extraction time (X1), extraction temperature (X2), and stirring rate (X6) exhibited a significant effect ($p < 0.1$) on the extraction process, as depicted in Figure 2. Furthermore, Table S5 shows the main effects estimated on the 2-MI and 4-MI and their *p*-values from the PB.

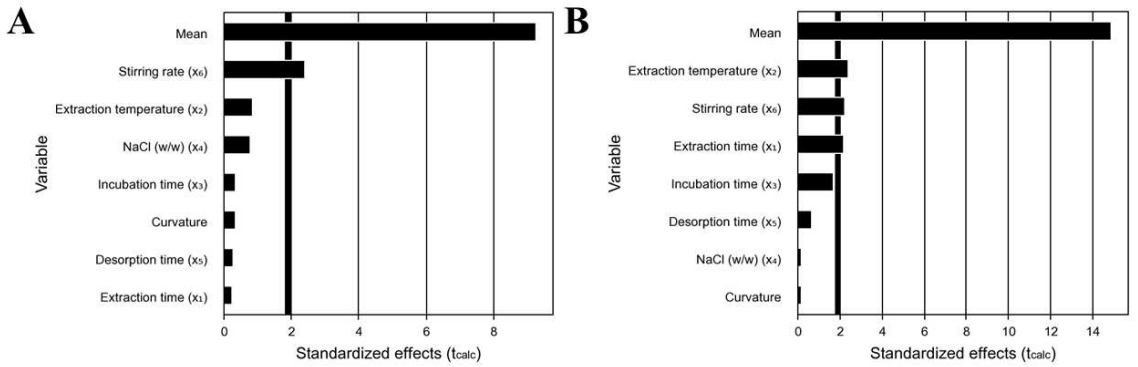

Figure 2. Pareto chart of the Plackett-Burman design response for 2-methylimidazole (A) and 4-methylimidazole (B).

The effect of extraction time (X_1) on the extraction capacity of both analytes was investigated. The results showed that this variable exhibited a positive effect on the extraction of 4-MI, implying that the extraction capacity increases as the extraction time is extended until equilibrium is reached (Oliveira et al., 2020; Souza-Silva & Pawliszyn, 2015). Furthermore, the extraction temperature (X_2) was another variable that exhibited

a positive effect on the extraction of 4-MI. The extraction temperature is associated with a decrease in viscosity which facilitates increased diffusivity of the analyte in the extract during the pre-equilibrium step. Another characteristic of this positive effect implies that an elevated temperature can enhance the extraction of analytes bound within the food matrix. Consequently, the analyte can transition into its free form in aqueous media (Oliveira et al., 2020; Souza-Silva & Pawliszyn, 2015).

The stirring rate (X_6) demonstrated a positive effect on the extraction of both analytes. An increase in the stirring rate can enhance mass transport phenomena, leading to improved diffusion of the analytes from the sample to the sorbent coating. Consequently, better agitation enhances the extraction response for these analytes (Souza-Silva & Pawliszyn, 2015).

Previous studies employed the PB method to evaluate the effects of the variables described earlier in this section using commercial fibers for extraction by SPME. Oliveira and co-workers reported that the extraction temperature and extraction time also exhibited a positive and significant effect on the extraction of volatile organic compounds using commercial fibers (Oliveira et al., 2020). Additionally, Souza-Silva and Pawliszyn observed that variables such as stirring rate and extraction temperature demonstrated a positive and significant effect on the extraction of certain pesticides (Souza-Silva & Pawliszyn, 2015). Upon investigating the Scopus database with the research terms ["Plackett-Burman" and "Polymeric Ionic Liquid" and "SPME"], no work was found utilizing PB for the optimization of extraction performance using PIL-based fibers.

Regarding the incubation time (X_3), no statistical significance was noted. This outcome suggests that prolonged exposure of the extract (in the extraction vial) to elevated temperatures could potentially disrupt the equilibrium conditions, negatively impacting the distribution coefficient of the analyte (K_{fs}) (Oliveira et al., 2020; Souza-

507 Silva & Pawliszyn, 2015). Although this parameter is more closely associated with the
508 headspace mode (HS) than the DI mode, the pre-incubation step must be executed to
509 ensure uniform temperature distribution throughout the sample vial and to mitigate
510 potential reproducibility issues (Souza-Silva & Pawliszyn, 2015). The shortest incubation
511 time employed in the PB experiment (5 min) was maintained for CCRD runs, without
512 adversely affecting the extraction efficiency.

513 The amount of NaCl (X_4) surprisingly did not yield any statistically significant
514 effect on any of the compounds under assessment. It was anticipated that NaCl might
515 enhance the extraction capacity in SPME through the salting-out effect, especially given
516 the high solubility of these analytes in water. Moreover, amines are generally susceptible
517 to the salting-out effect. A possible explanation for the obtained result could be linked to
518 the quantity of NaCl used. Excessive amounts of NaCl could potentially impact the
519 integrity of the fiber coatings, leading to damage. Consequently, a reduced number of
520 active sites may be available for extraction (Kataoka et al., 2000). As a result, the amount
521 of NaCl was set at the lowest level from the PB study (5% (0.750g) NaCl – w/v) to ensure
522 the longevity of the fiber without compromising extraction of the compounds.

523 In terms of desorption time (X_5), it can be stated that the desorption temperatures
524 used in the PB design demonstrated similar behavior for both analytes, and as a result,
525 did not have a statistically significant impact on the results. Thus, the desorption time was
526 fixed at 1 minute.

527 For the next optimization step (CCRD), independent variables that presented a
528 significant effect in the PB design were evaluated. Because the PB design is considered
529 to be saturated, its curvature is investigated through its central point. It is possible to
530 obtain lower or higher values in the other assays displayed in the PB screening. Thus, it
531 is assumed that a curvature can be created. Through the curvature test, it is therefore

possible to ascertain whether the statistically significant factors were disguised, either due to an increase in standard error or due to the *p*-value. Furthermore, this test can determine if the analysis was carried out using an ideal range, thereby making it a robust method.

It was found that the curvature for both analytes was not significant. This implies that curvature is not present in the central point area and that the variable ranges used in this screening were ideal for performing this design.

3.3.2. Central composite rotatable design (CCRD) and Derringer and Suich's tool

After identifying the independent variables through PB screening, a CCRD was executed to determine the optimal extraction conditions for both analytes. Consequently, due to the positive effects demonstrated by the selected variables in the PB screening, the range of each variable within the CCRD was expanded. The factor levels and experimental domain applied to the CCRD are displayed in Table S3. Furthermore, Table S4 illustrates the CCRD with both coded and real variables for the extraction of 2-MI and 4-MI in *açaí*-based food products.

Details for a new prediction model (reparametrized model), such as statistical coefficients, *p*-values, model fit, and regression significance, present ideal criteria for achieving good analytical performance (Table S6). In summary, the parametric models exhibited coefficients of determination of 93.56% and 94.75% for 2-MI and 4-MI, respectively, demonstrating that the values from the studied area yielded a good predictive model. Furthermore, the predictive model for both analytes did not exhibit a lack of fit; that is, it was not deemed significant, with values of 0.5114 and 0.2124 for 2-MI and 4-MI, respectively.

Since the studied compounds exhibited distinct optimal extraction conditions in the design of experiments (response surface methodology), as illustrated in Figure S6,

D&S were employed to attain the best simultaneous extraction response for both compounds. As a result, the algorithm proposed the following conditions: an extraction time of 100 minutes, an extraction temperature of 57.1 °C, and a stirring rate of 567 RPM. Moreover, these conditions exhibited a desirability score of 0.848. The model provided by D&S was experimentally confirmed in triplicate by comparing the predicted responses (peak area) with those obtained through experimentation, as shown in Table S7.

Lastly, it is worth noting that multivariate optimization improved the extraction capacity by 7 times when compared to non-optimized assays. This result confirms that the design of experiments (DoE) employed in this study was effective in enhancing the analytical response of the analytes.

3.4. In-house validation

The suitability of the PIL-based SPME method for the extraction of 2-MI and 4-MI in *açaí*-based food products was evaluated using the performance criteria displayed in Table 3. In addition, a representative chromatogram (Figure 3) and spectra (Figure S7), along with reference spectra (Figure S8) obtained from NIST, are provided in the supplementary material.

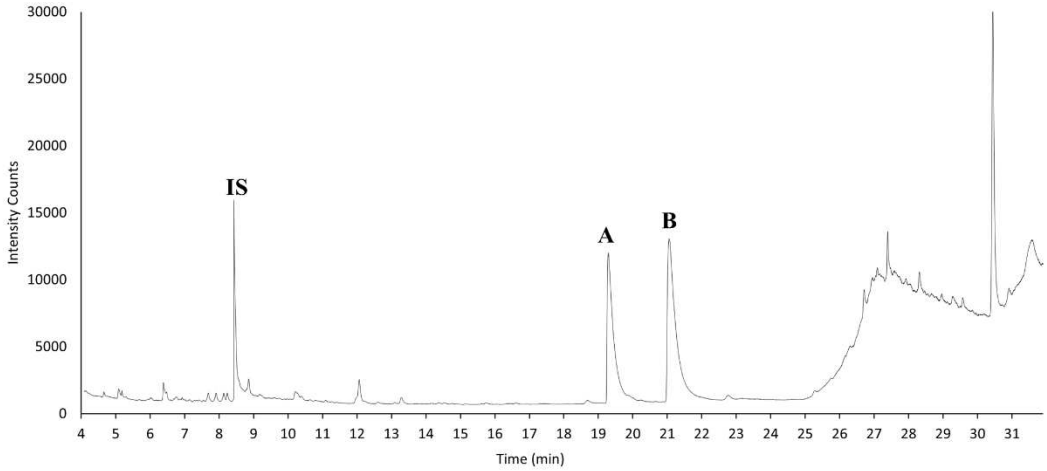

575

576 **Figure 3.** Representative chromatogram of a spiked sample with the internal standard
577 (IS), 2-methylimidazole (A), and 4-methylimidazole (B).

578

579 **Table 3**. Method performance characteristics obtained using the PIL based-SPME-GC-MS method.

Compound	LOD (µg kg^{-1})	LOQ (µg kg^{-1})	Linearity, R^2 (range of 75–200 µg kg^{-1})	Recovery (%, n = 3)			Precision, RSD % Intra-day, n = 3 (Inter-day, n = 9)			Matrix effect (%)
			Matrix-matched curve	75 µg kg^{-1}	100 µg kg^{-1}	200 µg kg^{-1}	75 µg kg^{-1}	100 µg kg^{-1}	200 µg kg^{-1}	
2-methylimidazole	25	75	0.9921	87.1	89.7	86.1	11.2 (8.6)	7.9 (7.1)	7.1 (7.6)	30
4-methylimidazole	25	75	0.9932	83.1	81.7	87.4	6.2 (9.2)	6.5 (9.8)	3.6 (8.3)	37

580 [a] water; LOD: limit of detection; LOQ: limit of quantification; R^2: coefficient of determination; RSD: relative standard deviation.

The LOD and LOQ values achieved the same limits for both analytes. The analytical limits met the criteria established by the food safety assessment agencies, namely EFSA and the European Commission, as well as the Cramer classification scheme. Due to the lack of specific regulations for limits on 2-MI and 4-MI in foodstuffs, the analytical method limits were established using the limits set for caramel colorants.

Signal enhancements were observed for both analytes. Due to complexities of the ingredients present in *açaí*-based food products, including macro and micronutrients and other organic compounds, the signal intensity can be affected (Nascimento et al., 2023). Thus, in order to mitigate the observed matrix effect, matrix-matched calibration curves were used for analytical quantification. Adequate linearity was obtained for both analytes with a coefficient of determination (R^2) ≥ 0.9921.

Repeatability (intra-day precision), reproducibility (inter-day precision), and recovery were employed to assess the extraction efficiency of the proposed method. The intra-day precision, expressed in terms of the relative standard deviation (RSD %), ranged from 7.1% to 11.2% for 2-MI and from 3.6% to 6.5% for 4-MI. In the case of the inter-day precision (RSD%), values between 7.1% and 8.6% for 2-MI and 8.3% and 9.8% for 4-MI were observed. Experimental results showed that the recovery for 2-MI ranged from 86.1% to 89.7%, and for 4-MI ranged from 83.1% to 87.4%. Precision and recovery tests comply with the performance criteria set by Commission Decision 2002/657/EC (EC, 2002). This commission established that the recovery test using a mass fraction ≥ 10 μg kg^{-1} shall have results between 80% and 110%, and the precision test for concentrations lower than 100 μg kg^{-1} shall have a coefficient of variation as low as possible.

3.5. Application and comparison of the method with others reported in the literature

606 Both secondary amines analyzed in this work represent a significant challenge in
607 sample preparation due to their chemical characteristics. In general, previous studies that
608 have investigated these amines require the use of long and laborious extraction processes,
609 such as a derivatization process (Cunha et al., 2016), or methods with low cost-
610 effectiveness, including employing single-use and expensive cartridges (Stone, 2017).
611 Due to their hydrophilic nature, they are not suitable for accurate determination by GC-
612 MS using a (5%-phenyl)-methylpolysiloxane phase capillary column (Cunha et al.,
613 2016). For this reason, the authors needed to derivatize these molecules to increase their
614 partition coefficient leading to improved performance upon analysis by GC-MS (Xu et
615 al., 2009). On the other hand, Cagliero et al. did not use a derivatization process when
616 analyzing acrylamide since they used a polar chromatographic stationary phase combined
617 with DI-SPME and a PIL-based fiber (Cagliero, Ho, et al., 2016). This analytical
618 technique was suitable for extracting polar analytes from food samples. Thus, in this
619 work, PIL-DI-SPME associated with a polar capillary column was used to avoid carrying
620 out the derivatization process. Additionally, due to the fact that 2-MI and 4-MI are low
621 volatility organic compounds and have low vapor pressure (0.01 [mmHg]) and high-water
622 solubility (PubChem, 2023), DI-SPME was chosen for performing this analysis.
623 Currently, the field of analytical chemistry has focused on green analysis,
624 avoiding the use of organic solvents. In an investigation on the Scopus database using the
625 terms “'2-methylimidazole' OR '4-methylimidazole' AND 'GC-MS'”, no paper was found
626 that has developed a method by GC-MS for food analysis without using organic solvents,
627 whether in the extraction, derivatization step, or pH correction of the extract. According
628 to this search, this is the first solvent-free method for the simultaneous analysis of 2-MI
629 and 4-MI in a food matrix using microextraction technique. Additionally, there are few
630 studies that investigate these analytes simultaneously. In summary, Table 4 shows a

631 comparison of the method developed in this study with others previously published in the
632 literature using the aforementioned terms in the Scopus database.

633 **Table 4.** Comparison of the method using PIL-based sorbent coatings and SPME-GC-MS with other GC-based methods.

Analyte	Sample	Extraction method	Use of organic solvents	Derivatization process*	Capillary column	Reference
4-MI	Brown colored foods and beverages	Ion-pair extraction	Yes (bis-2-ethylhexylphosphate, chloroform, hydrochloric acid, acetonitrile, isobutanol, pyridine, isobutyl chloroformate)	Yes	low-polarity (DB-5MS)	(Lee & Lee, 2016)
4-MI	Cooked meat	Solvent extraction	Yes (acetonitrile, isobutanol, pyridine, Isobutyl chloroformate, hexane)	Yes	mid-polarity (DB-35)	(Karim & Smith, 2015)
4-MI	Ammonia Caramel	Ion-pair extraction	Yes (bis(2-ethylhexyl) phosphoric acid, chloroform, hydrochloric acid, acetonitrile, isobutanol, pyridine, isobutyl chloroformate, isooctane).	Yes	low-polarity (RTX-5M)	(Wieczorek et al., 2018)
4-MI	Soluble coffee and coffee substitutes	Solvent extraction	Yes (methanol, bis-2-ethylhexylphosphate, chloroform, hydrochloric acid, acetonitrile, isobutanol, pyridine, isobutyl chloroformate)	Yes	low-polarity (DB-5MS)	(Cunha et al., 2016)

4-MI	Balsamic vinegars and processed sauces	Ion-pair extraction	Yes (bis-2-ethylhexylphosphate, chloroform, acetonitrile, isobutanol, pyridine, isobutyl chloroformate, isooctane)	Yes	low-polarity (DB-5MS)	(Cunha et al., 2014)
2-MI and 4-MI	*Açaí*-based food products	PIL-based SPME	No	no	high-polarity (HP-FFAP)	This work

* All derivatization procedures were based on the method using isobutyl chloroformate. 2-MI: 2-methylimdazole; 4-MI: 4-methylimidazole; PIL: polymeric ionic liquid; SPME: solid phase microextraction.

3.6. Occurrence of 2-methylimidazole and 4-methylimidazole in *açaí*-based food products

The validated method was applied to the evaluation of 2-MI and 4-MI in 25 samples of *açaí*-based food products (Table 1). 4-MI was quantified in samples B, E, and F at 79, 81, and 87 μg kg^{-1}, respectively. In sample S, 4-MI was detected below the LOQ. None of the samples showed 2-MI content above the LOD. Assuming that the formation of 2-MI is lower than the formation of 4-MI in foods (Wu et al., 2015), it was expected that 2-MI could have either low or no content in this matrix sample.

Finally, despite the quantified concentration being below the ADI established by EFSA and the European Commission's regulations, it is worth mentioning that the EFSA Panel on Food Additives and Nutrient Sources added to Food highlighted that the anticipated dietary exposure of child and adult populations may exceed the ADIs for caramels, including III and IV (EFSA, 2011). Thus, findings reported in this work can be useful for regulatory authorities to enhance the information on the food basket that contains 2-MI and 4-MI.

3.7. Practical aspects and green assessment of the analytical method

According to BAGI, it is recommended that a total score of 60 out of 100 be achieved so that the analytical procedure can be classified as a practical method (Manousi et al., 2023). Thus, the method developed in this work (PIL-based SPME-GC-MS) achieved sufficient parameters to be classified as an analytical approach that has practicality and applicability for use in routine analysis laboratories (Figure 4(A)). Furthermore, BAGI pictograms can comprise qualitative features based on different hues of dark blue, blue, light blue, and white, which represent high, medium, low, and no compliance with the method's practical criteria, respectively (Manousi et al., 2023).

Overall, BAGI can be considered as a complementary tool to other tools that assess the green capacity of an analytical method. In this case, a GABI tool was used to evaluate the green criteria, using pentagrams colored green, yellow, and red, representing low, medium, and high environmental impact, respectively (Płotka-Wasylka, 2018).

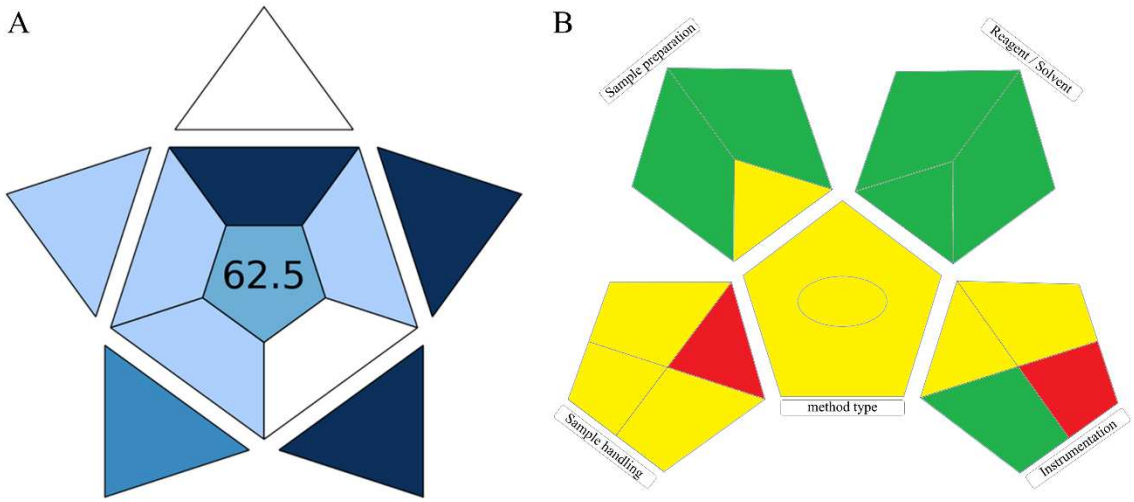

Figure 4. (A) Pictogram reflecting the aspects related to the practicality and applicability of the methodology by the Blue Applicability Grade Index (BAGI), and (B) pentagrams showing the environmental impact of the analytical procedure by the Green Analytical Procedure Index (GABI).

As depicted in Fig. 4(B), the GABI tool showed that the analytical method developed in this work had a low or medium environmental impact. The pictogram obtained predominantly highlighted in green and yellow, equivalent to 87% of the parts of all the pictograms, indicating a satisfactory analytical method. The category that ranked the use of solvents and reagents showed the best performance in the greenness assessment, with all parts of the pictogram marked in green. Regarding the red part in the sample handling pictogram, this classification was addressed to the collection topic of the sample. However, it must also be considered that for some analyses, it is not possible to

perform them on-site, as they require instruments only available in the laboratory. Thus, the significance of these green assessment tools lies in their ability to pinpoint additional vulnerabilities in the analytical process and contribute to the exploration of fresh, environmentally-friendly alternatives.

Lastly, the pictogram addressing the instrumentation assessment displayed one part classified in red color. This part refers to waste, which in this method generated around 15 mL of waste. However, it is worth highlighting that this waste comprised water, sample, and NaCl, which can undergo a recycling process.

4. Conclusions

An analytical method based on PIL-DI-SPME coupled to GC-MS was developed and fully validated for the simultaneous determination of 2-MI and 4-MI in *açaí*-based food products from Brazil and the United States. Three different PIL-based sorbent coatings were examined in this study and a commercial PA fiber was used for comparison purposes. Overall, the PIL-based fiber coating used in this work exhibited better extraction efficiency than commercial fiber when comparing their fiber volumes. Therefore, the PIL-based fiber was chosen to perform all optimized experiments, including the sequential multivariate optimization and analytical validation, due to its superior extraction efficiency compared to the others. DoE was able to increase the extraction capacity by 7 times as opposed to under non-optimized conditions. Validation criteria such as LOD, LOQ, linearity, recovery, matrix effects, and intra- and inter-days precision were evaluated to ensure the suitability of the analytical method. All validation parameters complied with the requirements of Commission Decision 2002/657/EC concerning performance of analytical methods. Furthermore, the extraction approach developed in this work for the analysis of 2-MI and 4-MI by GC-MS is novel since it did

not require the use of an organic solvent or a derivatization step. The validated method was applied to 25 samples, and 4-MI was identified in four samples ranging from < LOQ to 87 μg kg^{-1}. None of the samples showed a 2-MI content above the LOD. This is the first study using PIL-SPME coupled to GC-MS to identify and quantify 2-MI and 4-MI in food samples. It is expected that this data can be useful in the field of food quality control and can contribute to the knowledge of these contaminants in consumers' diets.

CRediT authorship contribution statement

Luis Eduardo Silva Nascimento: Conceptualization, Methodology, Software, Validation, Formal analysis, Investigation, Resources, Data curation, Writing - original draft, Writing - review & editing, Visualization. **Bhawana Thapa**: Methodology, Investigation, and Writing - review & editing. **Wellington da Silva Oliveira**: Conceptualization, Methodology, Software, Formal analysis, Resources, Writing - review & editing, and Supervision. **Plínio Ribeiro Rodrigues**: Software, Formal analysis, Resources, and Writing - Review & Editing. **Helena Teixeira Godoy**: Conceptualization, Methodology, Writing - review & editing, Supervision, Project administration, and Funding acquisition. **Jared L. Anderson**: Conceptualization, Methodology, Resources, Writing - review & editing, Visualization, Supervision, Project administration, and Funding acquisition.

Acknowledgments

This research was supported by the São Paulo Research Foundation (FAPESP) - grant#2021/11821-1; #2020/10990-1; #2020/02728-5. J.L.A. acknowledges support from the Chemical Measurement and Imaging Program at the National Science Foundation (CHE-2203891).

729

730 **Reference**

731 Akbari, N., Shafaroodi, H., Jahanbakhsh, M., Sabah, S., Molaee-aghaee, E., &
732 Sadighara, P. (2023). 4-Methylimidazole, a carcinogenic component in food,
733 amount, methods used for measurement; a systematic review. *Food Chemistry: X*,
734 *18*, 100739. https://doi.org/10.1016/J.FOCHX.2023.100739

735 Anderson, J. L., & Armstrong, D. W. (2005). Immobilized ionic liquids as high-
736 selectivity/high-temperature/high- stability gas chromatography stationary phases.
737 *Analytical Chemistry*, *77*(19), 6453–6462.
738 https://doi.org/https://doi.org/10.1021/ac051006f

739 Cagliero, C., Ho, T. D., Zhang, C., Bicchi, C., & Anderson, J. L. (2016). Determination
740 of acrylamide in brewed coffee and coffee powder using polymeric ionic liquid-
741 based sorbent coatings in solid-phase microextraction coupled to gas
742 chromatography–mass spectrometry. *Journal of Chromatography A*, *1449*, 2–7.
743 https://doi.org/10.1016/J.CHROMA.2016.04.034

744 Cagliero, C., Nan, H., Bicchi, C., & Anderson, J. L. (2016). Matrix-compatible sorbent
745 coatings based on structurally-tuned polymeric ionic liquids for the determination
746 of acrylamide in brewed coffee and coffee powder using solid-phase
747 microextraction. *Journal of Chromatography A*, *1459*, 17–23.
748 https://doi.org/10.1016/J.CHROMA.2016.06.075

749 Carriço, Í. R., Marques, J., Trujillo-Rodriguez, M. J., Anderson, J. L., & Rocha, S. M.
750 (2020). Sorbent coatings for solid-phase microextraction targeted towards the
751 analysis of death-related polar analytes coupled to comprehensive two-dimensional
752 gas chromatography: Comparison of zwitterionic polymeric ionic liquids versus
753 commercial coatings. *Microchemical Journal*, *158*, 105243.

https://doi.org/10.1016/J.MICROC.2020.105243

CONAB. (2021). *Conab - Histórico Mensal Açaí*. https://www.conab.gov.br/info-agro/analises-do-mercado-agropecuario-e-extrativista/analises-do-mercado/historico-mensal-de-acai

Cunha, S. C., Senra, L., Cruz, R., Casal, S., & Fernandes, J. O. (2016). 4-Methylimidazole in soluble coffee and coffee substitutes. *Food Control*, *63*, 15–20. https://doi.org/10.1016/J.FOODCONT.2015.11.006

Cunha, S. C., Senra, L., Fernandes, J. O., & Cunha, S. C. (2014). Gas Chromatography-Mass Spectrometry Analysis of 4-Methylimidazole in Balsamic Vinegars and Processed Sauces. *Food Analytical Methods*, *7*(7), 1519–1525. https://doi.org/10.1007/S12161-013-9782-6

Derringer, G., & Suich, R. (1980). Simultaneous Optimization of Several Response Variables. *Journal of Quality Technology*, *12*(4), 214–219. https://doi.org/10.1080/00224065.1980.11980968

EC, E. C. (2002). Commission Decision of 14 August 2002 implementing Council Directive 96/23/EC concerning the performance of analytical methods and the interpretation of results (notified under document number C(2002) 3044) (Text with EEA relevance) (2002/657/EC). *Official Journal of the European Communities*, *L 221*, 8. https://eur-lex.europa.eu/legal-content/EN/TXT/?uri=CELEX%3A02002D0657-20221128

EC, E. C. (2012). Commission Regulation (EU) No 231/2012 of 9 March 2012 laying down specifications for food additives listed in Annexes II and III to Regulation (EC) No 1333/2008 of the European Parliament and of the Council. *Official Journal of the European Communities*, *L83*, 1–295. https://eur-lex.europa.eu/legal-content/EN/TXT/?uri=CELEX%3A02012R0231-20230730

EFSA, E. F. S. A. (2011). Scientific Opinion on the re-evaluation of caramel colours (E 150 a,b,c,d) as food additives. *EFSA Journal*, *9*(3). https://doi.org/10.2903/j.efsa.2011.2004

Galindo, M. V., Oliveira, W. da S., & Godoy, H. T. (2021). Multivariate optimization of low-temperature cleanup followed by dispersive solid-phase extraction for detection of Bisphenol A and benzophenones in infant formula. *Journal of Chromatography A*, *1635*, 461757. https://doi.org/10.1016/J.CHROMA.2020.461757

Gionfriddo, E., Souza-Silva, É. A., Ho, T. D., Anderson, J. L., & Pawliszyn, J. (2018). Exploiting the tunable selectivity features of polymeric ionic liquid-based SPME sorbents in food analysis. *Talanta*, *188*, 522–530. https://doi.org/10.1016/J.TALANTA.2018.06.011

Hachuła, B., Nowak, M., & Kusz, J. (2010). Crystal and molecular structure analysis of 2-methylimidazole. *Journal of Chemical Crystallography*, *40*(3), 201–206. https://doi.org/https://doi.org/10.1007/s10870-009-9634-9

Ho, T. D., Canestraro, A. J., & Anderson, J. L. (2011). Ionic liquids in solid-phase microextraction: A review. *Analytica Chimica Acta*, *695*(1–2), 18–43. https://doi.org/10.1016/J.ACA.2011.03.034

Ho, T. D., Toledo, B. R., Hantao, L. W., & Anderson, J. L. (2014). Chemical immobilization of crosslinked polymeric ionic liquids on nitinol wires produces highly robust sorbent coatings for solid-phase microextraction. *Analytica Chimica Acta*, *843*, 18–26. https://doi.org/10.1016/J.ACA.2014.07.034

IARC. (2023). *List of Classifications – IARC Monographs on the Identification of Carcinogenic Hazards to Humans*. https://monographs.iarc.who.int/list-of-classifications

804 Joshi, M. D., Ho, T. D., Cole, W. T. S., & Anderson, J. L. (2014). Determination of
805 polychlorinated biphenyls in ocean water and bovine milk using crosslinked
806 polymeric ionic liquid sorbent coatings by solid-phase microextraction. *Talanta*,
807 *118*, 172–179. https://doi.org/10.1016/J.TALANTA.2013.10.014
808 Karim, F., & Smith, J. S. (2015). Detection and Quantification of 4(5)-Methylimidazole
809 in Cooked Meat. *Journal of Food Science*, *80*(2), T465–T471.
810 https://doi.org/10.1111/1750-3841.12748
811 Kataoka, H., Lord, H. L., & Pawliszyn, J. (2000). Applications of solid-phase
812 microextraction in food analysis. *Journal of Chromatography A*, *880*(1–2), 35–62.
813 https://doi.org/10.1016/S0021-9673(00)00309-5
814 Lee, S., & Lee, K. G. (2016). Analysis and risk assessment of 4(5)-methylimidazole in
815 brown colored foods and beverages. *Food Additives and Contaminants: Part B*
816 *Surveillance*, *9*(1), 59–65. https://doi.org/10.1080/19393210.2015.1127294
817 Manousi, N., Wojnowski, W., Płotka-Wasylka, J., & Samanidou, V. (2023). Blue
818 applicability grade index (BAGI) and software: a new tool for the evaluation of
819 method practicality. *Green Chemistry*, *25*(19), 7598–7604.
820 https://doi.org/10.1039/D3GC02347H
821 Meng, Y., Pino, V., & Anderson, J. L. (2011). Role of counteranions in polymeric ionic
822 liquid-based solid-phase microextraction coatings for the selective extraction of
823 polar compounds. *Analytica Chimica Acta*, *687*(2), 141–149.
824 https://doi.org/10.1016/J.ACA.2010.11.046
825 More, S. J., Bampidis, V., Benford, D., Bragard, C., Halldorsson, T. I., Hernández-
826 Jerez, A. F., Hougaard Bennekou, S., Koutsoumanis, K. P., Machera, K., Naegeli,
827 H., Nielsen, S. S., Schlatter, J. R., Schrenk, D., Silano, V., Turck, D., Younes, M.,
828 Gundert-Remy, U., Kass, G. E. N., Kleiner, J., … Wallace, H. M. (2019).

Guidance on the use of the Threshold of Toxicological Concern approach in food safety assessment. *EFSA Journal*, *17*(6). https://doi.org/10.2903/J.EFSA.2019.5708

Nacham, O., Clark, K. D., & Anderson, J. L. (2016). Extraction and Purification of DNA from Complex Biological Sample Matrices Using Solid-Phase Microextraction Coupled with Real-Time PCR. *Analytical Chemistry*, *88*(15), 7813–7820. https://doi.org/https://doi.org/10.1021/acs.analchem.6b01861

Nascimento, L. E. S., Wrona, M., da Silva Oliveira, W., Nerín, C., & Teixeira Godoy, H. (2023). A study on the migration of primary aromatic amines in packaged açaí-based (Euterpe oleracea Mart.) products. *Food Packaging and Shelf Life*, *38*, 101118. https://doi.org/10.1016/J.FPSL.2023.101118

Oliveira, W. da S., Monsalve, J. O., Nerin, C., Padula, M., & Godoy, H. T. (2020). Characterization of odorants from baby bottles by headspace solid phase microextraction coupled to gas chromatography-olfactometry-mass spectrometry. *Talanta*, *207*, 120301. https://doi.org/10.1016/J.TALANTA.2019.120301

Pacheco-Fernández, I., Najafi, A., Pino, V., Anderson, J. L., Ayala, J. H., & Afonso, A. M. (2016). Utilization of highly robust and selective crosslinked polymeric ionic liquid-based sorbent coatings in direct-immersion solid-phase microextraction and high-performance liquid chromatography for determining polar organic pollutants in waters. *Talanta*, *158*, 125–133. https://doi.org/10.1016/J.TALANTA.2016.05.041

Pacheco-Fernández, I., Trujillo-Rodríguez, M. J., Kuroda, K., Holen, A. L., Jensen, M. B., & Anderson, J. L. (2019). Zwitterionic polymeric ionic liquid-based sorbent coatings in solid phase microextraction for the determination of short chain free fatty acids. *Talanta*, *200*, 415–423.

https://doi.org/10.1016/J.TALANTA.2019.03.073

Pedersen-Bjergaard, S. (2019). Analytical microextraction – Present status and future directions. *TrAC Trends in Analytical Chemistry*, *118*, 770. https://doi.org/10.1016/J.TRAC.2019.07.004

Płotka-Wasylka, J. (2018). A new tool for the evaluation of the analytical procedure: Green Analytical Procedure Index. *Talanta*, *181*, 204–209. https://doi.org/10.1016/J.TALANTA.2018.01.013

PubChem. (2023). *PubChem*. https://pubchem.ncbi.nlm.nih.gov/

Revelou, P. K., Xagoraris, M., Alissandrakis, E., Pappas, C. S., & Tarantilis, P. A. (2021). A Review of the Analytical Methods for the Determination of 4(5)-Methylimidazole in Food Matrices. *Chemosensors 2021, Vol. 9, Page 322*, *9*(11), 322. https://doi.org/10.3390/CHEMOSENSORS9110322

Shirey, R. E. (2012). SPME Commercial Devices and Fibre Coatings. In J. Pawliszyn (Ed.), *Handbook of Solid Phase Microextraction* (pp. 99–133). Elsevier. https://doi.org/10.1016/B978-0-12-416017-0.00004-8

Souza-Silva, É. A., & Pawliszyn, J. (2015). Direct immersion solid-phase microextraction with matrix-compatible fiber coating for multiresidue pesticide analysis of grapes by gas chromatography-time-of-flight mass spectrometry (DI-SPME-GC-ToFMS). *Journal of Agricultural and Food Chemistry*, *63*(18), 4464–4477. https://doi.org/https://doi.org/10.1021/jf506212j

Stone, J. (2017). Sample preparation techniques for mass spectrometry in the clinical laboratory. In H. Nair & C. William (Eds.), *Mass Spectrometry for the Clinical Laboratory* (pp. 37–62). Academic Press. https://doi.org/10.1016/B978-0-12-800871-3.00003-1

Wieczorek, M. N., Przygoński, K., & Jeleń, H. H. (2018). Determination of 4-

879 Methylimidazole in Ammonia Caramel Using Gas Chromatography-Tandem Mass
880 Spectrometry (GC-MS/MS). *Journal of Food Quality*, *2018*.
881 https://doi.org/10.1155/2018/4696074
882 Xu, L., Basheer, C., & Lee, H. K. (2009). Chemical reactions in liquid-phase
883 microextraction. *Journal of Chromatography A*, *1216*(4), 701–707.
884 https://doi.org/10.1016/J.CHROMA.2008.10.005
885 Yu, H., Ho, T. D., & Anderson, J. L. (2013). Ionic liquid and polymeric ionic liquid
886 coatings in solid-phase microextraction. *TrAC Trends in Analytical Chemistry*, *45*,
887 219–232. https://doi.org/10.1016/J.TRAC.2012.10.016
888 Yu, H., Merib, J., & Anderson, J. L. (2016). Crosslinked polymeric ionic liquids as
889 solid-phase microextraction sorbent coatings for high performance liquid
890 chromatography. *Journal of Chromatography A*, *1438*, 10–21.
891 https://doi.org/10.1016/J.CHROMA.2016.02.027
892 Zeger, V. R., Bell, D. S., Herrington, J. S., & Anderson, J. L. (2022). Selective isolation
893 of pesticides and cannabinoids using polymeric ionic liquid-based sorbent coatings
894 in solid-phase microextraction coupled to high-performance liquid
895 chromatography. *Journal of Chromatography A*, *1680*, 463416.
896 https://doi.org/10.1016/J.CHROMA.2022.463416
897